Video Article

A Polished and Reinforced Thinned-skull Window for Long-term Imaging of the Mouse Brain

Andy Y. Shih[1], Celine Mateo[1], Patrick J. Drew[2,3], Philbert S. Tsai[1], David Kleinfeld[1,4]

[1]Department of Physics, University of California, San Diego
[2]Department of Engineering Science and Mechanics, Pennsylvania State University
[3]Department of Neurosurgery, Pennsylvania State University
[4]Section of Neurobiology, University of California, San Diego

Correspondence to: Andy Y. Shih at a2shih@ucsd.edu

URL: http://www.jove.com/video/3742/
DOI: 10.3791/3742

Keywords: Neuroscience, Issue 61, cranial window, craniotomy, two-photon microscopy, blood flow, dendrite, optogenetics, cortex, capillary, microglia, chronic, mouse,

Date Published: 3/7/2012

Citation: Shih, A.Y., Mateo, C., Drew, P.J., Tsai, P.S., Kleinfeld, D. A Polished and Reinforced Thinned-skull Window for Long-term Imaging of the Mouse Brain. J. Vis. Exp. (61), e3742, DOI : 10.3791/3742 (2012).

Abstract

In vivo imaging of cortical function requires optical access to the brain without disruption of the intracranial environment. We present a method to form a polished and reinforced thinned skull (PoRTS) window in the mouse skull that spans several millimeters in diameter and is stable for months. The skull is thinned to 10 to 15 μm in thickness with a hand held drill to achieve optical clarity, and is then overlaid with cyanoacrylate glue and a cover glass to: 1) provide rigidity, 2) inhibit bone regrowth and 3) reduce light scattering from irregularities on the bone surface. Since the skull is not breached, any inflammation that could affect the process being studied is greatly reduced. Imaging depths of up to 250 μm below the cortical surface can be achieved using two-photon laser scanning microscopy. This window is well suited to study cerebral blood flow and cellular function in both anesthetized and awake preparations. It further offers the opportunity to manipulate cell activity using optogenetics or to disrupt blood flow in targeted vessels by irradiation of circulating photosensitizers.

Video Link

The video component of this article can be found at http://www.jove.com/video/3742/

Protocol

1. Preparing for Surgery [i]

1. Clean the surgical tools by sonicating in a mixture of Maxizyme and Surgical Milk in an ultrasonic cleaner. Autoclave the surgical tools before each experiment.
2. Ensure that all necessary reagents and disposables are available. A list of reagents and disposables is provided in Table 2. Reagents and disposables that come in contact with exposed tissue should be sterile, when possible.
3. Induce anesthesia. Typical anesthetics suitable for survival studies are described in Table 1. Ensure surgical plane of anesthesia by checking for lack of toe pinch reflex. The optimal age of mouse is 3 to 6 weeks of age. The skulls of younger mice are softer and more difficult to thin. Older mice have thicker skulls that will bleed more during the thinning procedure.
4. Secure the animal in a stereotaxic frame [1]. A list of surgical equipment is provided in Table 2.
5. Maintain body temperature at 37°C using a feedback regulated rectal probe and heat pad.
6. Apply ophthalmic ointment to the eyes to retain moisture.
7. Shave the scalp with a small electrical razor.
8. Clean the scalp with Betadine, followed by swabbing with 70 % (v/v) isopropyl alcohol.
9. If desired, check that heart and breathing rates are within a normal range using a pulse oximeter. For a mouse, these numbers should center around 10 and 2 Hz, respectively.
10. Warm an aliquot of sterile-filtered artificial cerebral spinal fluid (ACSF) to 37°C (125 mM NaCl, 10 mM glucose, 10 mM HEPES, 3.1 mM $CaCl_2$, 1.3 mM $MgCl_2$, pH 7.4) (all chemicals from Sigma)[2].

2. Mounting a Head Frame

1. Remove the scalp over the entire dorsal skull surface with a pair of forceps and surgical scissors. Trim the skin laterally to the edges of the temporal muscles on either side of the skull and posterior to the muscles of the neck (**Fig. 1A**).
2. Use a scalpel blade to remove the thin periosteum from the surface of the skull.
3. Clean the skull with a moist cotton tipped applicator and dry the skull surface with a stream of air from a dust can. Then apply a thin layer of cyanoacrylate glue to the entire skull surface. Allow the glue to dry thoroughly. This layer of glue is required for proper adherence of the dental cement in subsequent steps. The cyanoacrylate glue does not need to be sterilized.
4. Attach a metal connector to the skull surface, away from the area of the desired window. For anesthetized preparations, a small nut may be secured to the skull with a dab of cyanoacrylate glue, which can later be screwed into the imaging setup using a bolt (**Fig. 1B, 1L and 1N**).

Seal the backside of the nut with tape to ensure that glue does not enter the threads during attachment to the skull. The nut and tape should be sterilized by autoclaving prior to the surgery.

5. For awake imaging preparations, attach a more rigid custom connector with two attachment points (**Fig. 1M and 1N**). Drill two holes in the skull over the contralateral cortical hemisphere with a ½ mm drill burr, and then introduce two #000 self-tapping screws. These screws will help anchor the head mount to the skull. Apply only one full turn of the screw, in order to avoid applying pressure to the underlying cortex. Then, attach the custom metal cross bar with a small dab of cyanoacrylate glue over the cerebellum. Allow the cyanoacrylate glue to dry thoroughly. This metal connector greatly reduces the degrees of freedom and simplifies relocation of the same imaging field in longitudinal studies. A wide cross bar gives ample room for electrode placement and stimulation of vibrissae. Detailed plans for generating the custom head mount and attachment device are available online (http://physics.ucsd.edu/neurophysics/links.html). The screws and cross bar should be sterilized by autoclaving prior to the surgery.
6. Cover the entire skull surface, excluding the location of the window, with a layer of dental cement (**Fig. 1C and 1D**). Ensure that all exposed edges of the skin are covered by cement. The components of the dental cement do not need to be sterilized.

3. The Generation of a Polished and Reinforced Thinned-skull (PoRTS) Window

1. Ensure that drill burrs are sharp and avoid reusing them. Using a low speed on the dental drill, thin a 2 mm by 2 mm region over the somatosensory cortex with a ½ mm burr. Alternate between wetting the skull with ACSF and then drying the skull surface with a gentle stream of air from a gas duster; wet for cooling, and dry for thinning. This requires thinning through the cancellous layer of the skull, which may bleed, but can be controlled by flushing with ACSF (**Fig. 1E**). The skull begins to flex under the slight pressure of the drill when it is ~50 µm, and the pial vessels should be visible through wet bone (**Fig. 1F**). At this thickness, small white spots within the bone will become visible for a few seconds immediately after the dry skull surface is moistened.
2. At this point, thin the bone even further. Use a slower drill speed, i.e., 1000 rpm, which shaves the skull surface with only a slight touch. Use small controlled movements while holding the drill like a pen and only apply force in the lateral direction. The bone should be ~10 to 15 µm at its final thickness (**Fig. 1G**). When the bone is sufficiently thin, the small white spots in the bone will no longer be visible when the dry skull surface is moistened.
3. Polish the window region with tin oxide powder. Attach a pre-made drill bit that has been dipped in silicone aquarium sealant and withdrawn, leaving a tapered whip (**inset, Fig. 1H**). The silicone whip should be prepared at least one day before the surgery, and sterilized with 70% isopropanol prior to use. Place a small pinch of powder on the window along with a drop of ACSF (**Fig. 1H**). Agitate the slurry over the window for up to ten minutes by gently touching the tip of the moving whip to the skull surface. Flush away the tin oxide powder thoroughly from the window using ACSF and dry the bone thoroughly with a gentle stream of air. Surface irregularities and adherent bone chips left by drilling in the previous steps should be removed after polishing (**Fig. 1H and 1I**). The tin oxide powder does not need to be sterilized.
4. Cut square pieces of no. 0 cover glass slightly smaller than the size of the window. Use a scribe to gently score separated horizontal and vertical lines in the cover slip using a straight edge. Then place the cover slip in a petri dish and knock the dish against a table edge to separate the glass pieces. The entire petri dish can then be autoclaved to ensure sterility.
5. Place an appropriately sized cover glass nearby the dried window. Apply a small dab of cyanoacrylate glue over the window using the tip of a broken wooden cotton tip applicator, and quickly push the precut piece of cover glass atop the glue. Avoid creating bubbles underneath the cover glass. Gently push the cover glass against the skull surface, and hold for a few seconds (**Fig. 1J and 1O**). Allow the glue to dry thoroughly over 15 minutes. Excess cyanoacrylate glue can be removed from the upper surface of the cover glass with a scalpel blade after it is dried. Seal the edges of the cover glass with dental cement and form a slightly raised well to hold water for the dipping lens (**Fig. 1K and 1O**).

4. Recovery

1. Place the animal in a warm cage following surgery. Monitor the animal periodically until it fully recovers from anesthesia.
2. If the preparation is meant to survive for more than one day, provide buprenorphine (0.03 µg per g rodent) for analgesia. We typically image the animal at least one day after the initial implantation.

5. Imaging Preparation

1. Stabilize the animal on an optical breadboard for imaging, using the frame as a head support (**Fig. 1L and 1M**). A restraint apparatus can be made from commercially available optomechanical components from Qioptiq or ThorLabs. Our separate plate can be transported between surgical and two-photon imaging suites with the animal and all physiological monitoring devices assembled as one unit [3].
2. If blood flow imaging is desired, inject 0.05 mL of 5% (w/v) fluorescent-dextran dye dissolved in sterile saline either through the tail vein or infraorbital vein to label the blood serum (**Fig. 2A and 2C to 2H**) [4-7]. This must be done under general anesthesia. Infraorbital vein administration may be easier for beginners, as dextran solutions are more viscous. The tail vein can be difficult to locate in dark colored mice, and the vein tends to collapse after a failed injection. For imaging vasculature with green emission, use a fluorescein isothiocyanate dextran. For red emission, use a Texas Red dextran. With high molecular weight dextrans, the dye will remain in circulation for several hours. Alternatively, animals with endogenous fluorescent labels can be imaged directly at the appropriate two-photon excitation wavelength. The dextran solution can be frozen in aliquots for future use.
3. Gently clean the window surface with a moist cotton tipped applicator.
4. For prolonged imaging of anesthetized preparations, inject sterile lactated Ringer's solution intraperitoneally at a volume of 3 µL per gram every 2 hours to maintain body fluids and energy requirements.
5. When imaging animals in the awake state, limit head restraint to only a few hours at a time to reduce stress levels. Return the animal to the home cage between imaging sessions for food and water.

6. Representative Results

A successful window will allow imaging depths up to 250 µm below the pial surface for several months. This method has been used to study *in vivo* capillary blood flow [4, 8], microglial activation [8, 9], and dendritic structure within the cortical parenchyma [8]. In one example, we use two-photon imaging to show the cortical vasculature of an anesthetized Thy1-yellow fluorescent protein (YFP) mouse, after the blood serum is labeled by intravenous injection of Texas Red dextran (**Fig. 2A**). Dural vessels are often visible slightly above the cortical surface in the dura mater (**Fig. 2C, arrow**). Large pial arterioles and venules lie on the cortical surface **(Fig 2D**). Penetrating vessels branch from this surface network and dive into the cortex where they ramify into a dense capillary bed that feeds the cortical tissue (**Fig. 2E to 2H**). Dendritic arbors of deep YFP expressing

cortical neurons, a signal endogenous to this mouse line, can be imaged concurrently in a second channel [10] (**Fig. 2B to 2H**). The second harmonic signal of the bone was collected in a third channel, and can be used to gauge the thickness of the thinned skull after collection of image stacks (**Fig. 2A to 2C**).

Cortical vascular dynamics are profoundly affected by anesthetics [11]. In a second example, we show a video of spontaneous vasoactivity collected by two-photon microscopy from a habituated awake mouse. Prominent vasomotor oscillations in the lumen diameter are seen with a pial arteriole, but not with a neighboring venule. This basal range of vasoactivity is diminished with urethane anesthesia [4]. To quantify spontaneous and evoked changes in blood flow, we use adapted line scanning techniques to capture both the vascular diameter and red blood cell velocity of individual vessels. Detailed resources on quantitative blood flow imaging using two-photon microscopy are available [3, 12].

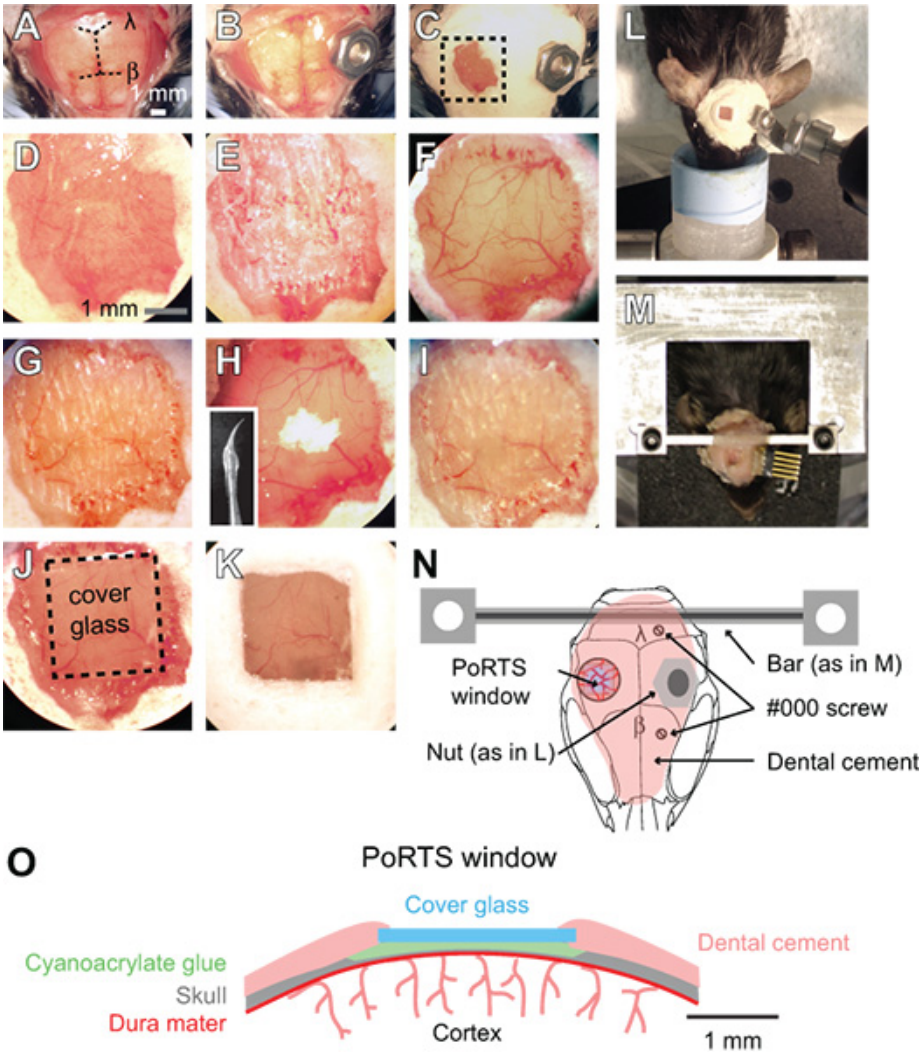

Figure 1. Procedure for a PoRTS window. (A to K) Images of sequential steps in the procedure for generating a PoRTS window. See text for detailed instructions. β = bregma and λ = lambda. (**L**) Bolt and nut system for securing the head during imaging of anesthetized preparations. (**M**) Custom machined cross bar head mount for awake preparations. In this example, a connector was also implanted for repeated electrocorticogram recordings. (**N**) Schematic diagram showing dorsal view of the head mount and position of various components. The nut used in panel L is meant as alternative to the cross bar using in panel M. Two #000 self-tapping screws are added with the cross bar mount for added stability with awake imaging preparations. (**O**) Schematic diagram showing cross section of a PoRTS window.

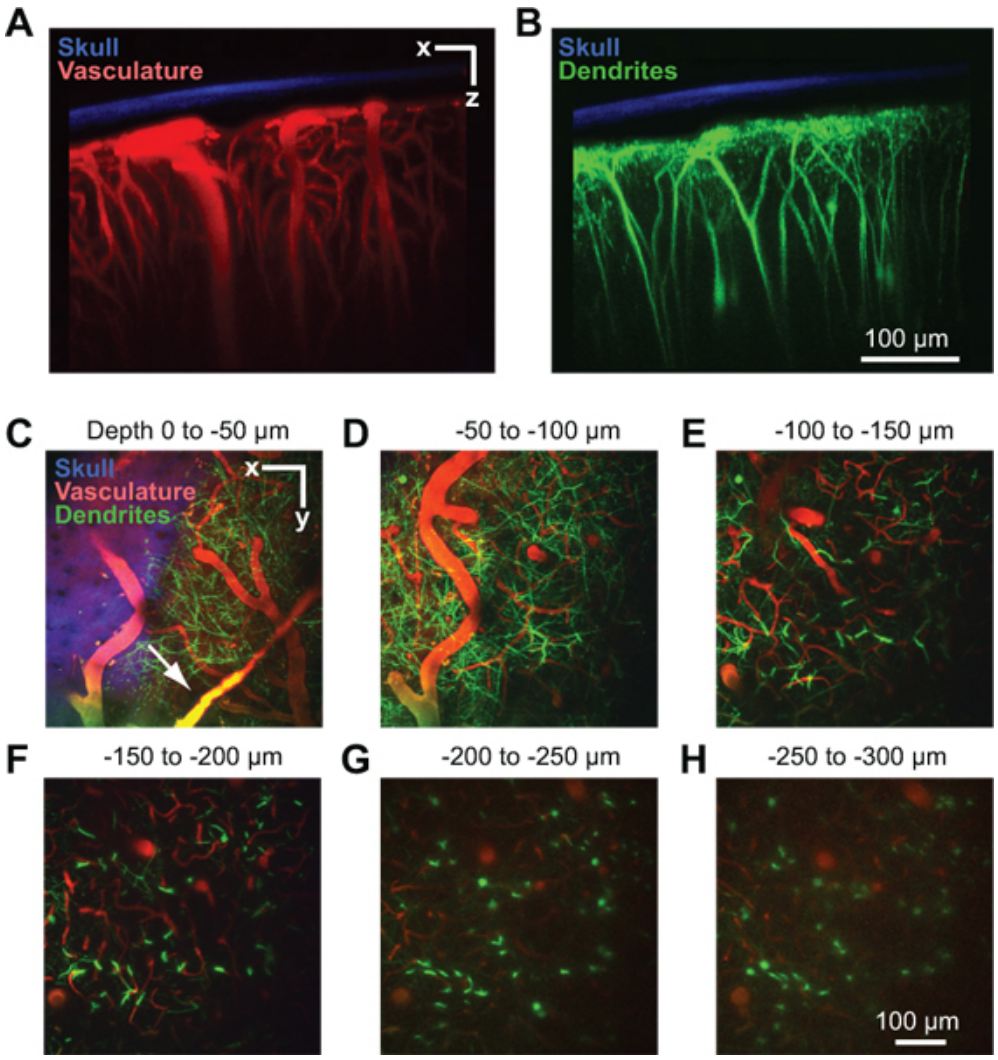

Figure 2. Two-photon imaging of vasculature and neuronal structure in mouse cortex. All images were collected through a PoRTS window in a Thy1-YFP mouse at 2 days after window implantation [10]. Maximal projection over 150 µm of tissue in the coronal orientation showing the thinned skull in relation to the vasculature (**A**) and dendrites (**B**). The bone (blue) was detected by collecting the second harmonic fluorescence at 450 nm emission with 900 nm excitation [8]. The vasculature (red) was labeled by intravenously injected 70 kDa Texas Red dextran [6]. The dendritic fields of neurons (green) are endogenous to the Thy1-YFP transgenic mouse line. (**C-H**) Maximal projections over 50 µm of tissue in the horizontal orientation at different depths below the pia. Data is from the same image stack shown in Panels A and B. Dural vessels may be visible just above the cortical surface (**arrow in C**).

Abbreviations

ACSF = artificial cerebral spinal fluid

PoRTS = polished and reinforced thinned skull window

YFP = yellow fluorescent protein

[i]Ensure that the procedures described are approved by your local Institutional Animal Care and Use Committee.

Discussion

Two-photon imaging through a PoRTS window requires transmission through the thinned bone and the dura, which attenuates the laser light and adds optical aberrations at greater depths [8]. However, despite this drawback, imaging depths up to 250 µm below the pial surface can be achieved with 900 nm excitation. Greater imaging depths may in principle be possible with longer excitation wavelengths [13]. A major advantage of this method is the absence of cortical inflammation that might exist transiently in methods involving full craniotomy [14, 15]. A well prepared PoRTS window should show no overt signs of angiogenesis or inflammation following implantation [8]. This may be assessed *in vivo* during the course of the experiment by imaging vasculature structure, or by detecting morphological changes of microglia in the CX(3)CR1-GFP mouse line [8, 16, 17]. Further, *post hoc* immunohistology should be performed to confirm the absence of astrogliosis in the superficial cortex, for example, using an antibody for glial fibrillary acidic protein [8].

The most demanding step in generating a PoRTS window is thinning the bone to 10 to 15 µm in thickness. Periodic examination of the window under a wide field fluorescence dissection microscope is also useful to gauge skull thickness during the thinning procedure. Fluorescent labels near the cortical surface should be clearly visible through the wet skull. For a more accurate measure of skull thickness, the second harmonic signal from the bone can be measured in a three-dimensional stack under two-photon microscopy (**Fig. 2A to 2C**). If this is done prior to

application of the glue and cover glass, the bone and can be further thinned if necessary. Insufficient thinning results in poor imaging depth. Polishing will continue to thin the skull when drilling is no longer possible, and will help reduce surface irregularities and adherent bone chips. In preliminary studies, we have found that polishing improves imaging depth weeks after the initial implantation. However, a rigorous analysis on the benefit of polishing has not been performed.

The application of cyanoacrylate glue and cover glass atop the bone is a critical step to reduce light scattering and allow for deeper imaging. Due to the drilling process, the surface of the bone will be irregular, even after polishing, and therefore light scattering. The application of cyanoacrylate glue fills in these irregularities and the overlying cover glass leaves a non-scattering smooth surface. Importantly, the refractive indices for the glue and cover glass, which are 1.45 and 1.52 according to manufacturer specifications, are closely indexed matched to that of bone at 1.55 [18]. This is an improvement over having air or water above the thinned skull, which have refractive indices of 1.00 and 1.33. Critically, the cyanoacrylate glue further helps to impede bone re-growth. This enables longitudinal imaging for up to three months, without the need for additional maintenance after the initial surgery.

A second cause of poor imaging depth is damage to pial vessels leading to hemorrhaging or edema. Vibrations from the drill should be minimized. In a small proportion of cases, bleeding within the dura will be unavoidable. This is because the vasculature of the dura mater is continuous with the vascular plexus of the skull, which is disturbed during the thinning procedure. Preparations with any sign of sub-dural bleeding should be discarded as dural thickening and angiogenesis will ensue. The success rate of the PoRTS window can be as high as 80% with practice.

For some experiments, it may be necessary to inject dyes/viruses or insert electrodes into the tissue beneath the PoRTS window. It is possible to generate a small hole adjacent to the window, through which pipettes or electrodes can be introduced using a stereotaxic arm or Sutter manipulator [19]. This hole can be resealed with bone wax if the animal is to be imaged again in future sessions. However, the introduction of electrodes can of course lead to inflammation in the cortex and acute pathology such as spreading depression.

The PoRTS window should be well suited for any imaging modality requiring optical access to the brain. This includes surface imaging techniques such as intrinsic optical imaging [20] and laser speckle imaging [21], or optical sectioning techniques such as confocal [22] or two-photon microscopy [23]. Further, a PoRTS preparation should improve resolution in wide field transcranial imaging techniques such as optical coherence tomography [24] and photoacoustic microscopy [25].

Finally, the PoRTS window is suitable for imaging of awake animals as the cover glass adds rigidity to the window [4]. The head mount is further stabilized by the introduction of two self-tapping #000 screws to the contralateral hemisphere prior to application of the dental cement (**Fig. 1L**). Habituation to head-fixation is important to reduced animal movement during imaging. A new animal can be gradually accustomed to head-restraint over a period of 3 to 7 days prior to imaging, starting with 15 min sessions and working up to several hours.

Disclosures

Nothing to disclose.

Acknowledgements

This work was supported by the American Heart Association (Post-doctoral fellowship to AYS) and the National Institutes of Health (MH085499, EB003832, and OD006831 to DK). We thank Beth Friedman and Pablo Blinder for comments on the manuscript.

References

1. Cetin, A., *et al.* Stereotaxic gene delivery in the rodent brain. *Nature Protocols.* **1**, 3166-3173 (2006).
2. Kleinfeld, D. & Delaney, K.R. Distributed representation of vibrissa movement in the upper layers of somatosensory cortex revealed with voltage sensitive dyes. *Journal of Comparative Neurology.* **375**, 89-108 (1996).
3. Driscoll, J.D., *et al.* Quantitative two-photon imaging of blood flow in cortex. In: Imaging in Neuroscience and Development. Yuste, R., ed., Cold Spring Harbor Laboratory Press, New York, 927-37 (2011).
4. Drew, P.J., Shih, A.Y., & Kleinfeld, D. Fluctuating and sensory-induced vasodynamics in rodent cortex extends arteriole capacity. *Proceedings of the National Academy of Sciences U.S.A.* **108**, 8473-8478 (2011).
5. Mostany, R. & Portera-Cailliau, C. A Method for 2-Photon Imaging of Blood Flow in the Neocortex through a Cranial Window. *J. Vis. Exp.* (12), e678, DOI: 10.3791/678 (2008).
6. Zhang, S., *et al.* Rapid reversible changes in dendritic spine structure *in vivo* gated by the degree of ischemia. *Journal of Neuroscience*. **25**, 5333-5338 (2005).
7. Takano, T., *et al.* Astrocyte-mediated control of cerebral blood flow. *Nature Neuroscience*. **9**, 260-267 (2006).
8. Drew, P.J., *et al.* Chronic optical access through a polished and reinforced thinned skull. *Nature Methods*. **7**, 981-984 (2010).
9. Marker, D.F., *et al.* A thin-skull window technique for chronic two-photon *in vivo* imaging of murine microglia in models of neuroinflammation. *Journal of Visualized Experiments.* **19** (43), e2059 (2010).
10. Feng, G., *et al.* Imaging neuronal subsets in transgenic mice expressing multiple spectral variants of GFP. *Neuron.* **28**, 41-51 (2000).
11. Martin, C., *et al.* Investigating neural-hemodynamic coupling and the hemodynamic response function in the awake rat. *Neuroimage.* **32**, 33-48 (2006).
12. Shih, A.Y., *et al.* Two-photon microscopy as a tool to study blood flow and neurovascular coupling in the rodent brain. *Journal of Cerebral Blood Flow and Metabolism.*, In press, (2011).
13. Kobat, D., *et al.* Deep tissue multiphoton microscopy using longer wavelength excitation. *Optics Express.* **17**, 13354-13364 (2009).
14. Holtmaat, A., *et al.* Long-term, high-resolution imaging in the mouse neocortex through a chronic cranial window. *Nature Protocols.* **4**, 1128-1144 (2009).
15. Xu, H.T., *et al.* Choice of cranial window type for *in vivo* imaging affects dendritic spine turnover in the cortex. *Nature Neuroscience.* **10**, 549-551 (2007).
16. Nimmerjahn, A., Kirchhoff, F., & Helmchen, F. Resting microglial cells are highly dynamic surveillants of brain parenchyma *in vivo*. *Science.* **308** (5726), 1314-1318 (2005).
17. Davalos, D., *et al.* ATP mediates rapid microglial response to local brain injury *in vivo*. *Nature Neuroscience*. **8**, 752-758 (2005).

18. Ascenzi, A. & Fabry, C. Technique for dissection and measurement of refractive index of osteons. *The Journal of Biophysical and Biochemical Cytology.* **6**, 139-142 (1959).
19. Stosiek, C., *et al. In vivo* two-photon calcium imaging of neuronal networks. *Proceedings of the National Academy of Sciences U.S.A.* **100**, 7319-7324 (2003).
20. Grinvald, A., *et al.* Functional architecture of cortex revealed by optical imaging of intrinsic signals. *Nature.* **324**, 361-364 (1986).
21. Dunn, A.K., *et al.* Dynamic imaging of cerebral blood flow using laser speckle. *Journal of Cerebral Blood Flow & Metabolism.* **21**, 195-201 (2001).
22. Villringer, A., *et al.* Capillary perfusion of the rat brain cortex: An *in vivo* confocal microscopy study. *Circulation Research.* **75**, 55-62 (1994).
23. Denk, W., Strickler, J.H., & Webb, W.W. Two-photon laser scanning fluorescence microscopy. *Science.* **248**, 73-76 (1990).
24. Srinivasan, V.J., *et al.* Optical coherence tomography for the quantitative study of cerebrovascular physiology. *Journal of Cerebral Blood Flow & Metabolism.* **31** (6), 1339-1345 (2011).
25. Hu, S. & Wang, L.V. Photoacoustic imaging and characterization of the microvasculature. *Journal of Biomedical Optics.* **15**, 011101 (2010).
26. Flecknell, P.A. Laboratory animal anesthesia. San Diego, Academic Press, (1987).

